

# Regulation of ERK1/2 and SMAD2/3 Pathways by Using Multi-Layered Electrospun PCL–Amnion Nanofibrous Membranes for the Prevention of Post-Surgical Tendon Adhesion

This article was published in the following Dove Press journal:  
*International Journal of Nanomedicine*

Chunjie Liu<sup>1,\*</sup>

Siyu Tian<sup>2,\*</sup>

Jiangbo Bai<sup>2</sup>

Kunlun Yu<sup>2</sup>

Lei Liu<sup>3</sup>

Guoli Liu<sup>4</sup>

Ruiyi Dong<sup>5</sup>

Dehu Tian<sup>2</sup>

<sup>1</sup>Department of Orthopedics, Tangshan Workers Hospital, Tangshan, Hebei 063000, People's Republic of China;

<sup>2</sup>Department of Hand Surgery, The Third Affiliated Hospital of Hebei Medical University, Shijiazhuang, Hebei 050051, People's Republic of China; <sup>3</sup>Department of Orthopedics, Changping District Hospital, Beijing 102200, People's Republic of China; <sup>4</sup>Department of Orthopedics, The Second Hospital of Tangshan, Tangshan, Hebei 063000, People's Republic of China; <sup>5</sup>Department of Orthopedics, Cangzhou Integrated Traditional Chinese and Western Medicine Hospital, Cangzhou, Hebei 061001, People's Republic of China

\*These authors contributed equally to this work

**Background:** Adhesion after tendon injury is a common complication in clinical practice. The lack of effective prevention mechanisms seriously affects the functional rehabilitation of patients. This research aimed to optimise the amniotic membrane and explain the mechanism of tendon–amniotic membrane by imitating the tendon sheath to construct a multilayer electrospun polycaprolactone (PCL) nanofibre membrane.

**Materials and Methods:** Fresh amnions were subjected to freezing and vacuum drying. The two surfaces of freeze-dried amnions were coated with PCL nanofibres by electrospinning, thereby forming a multilayer composite membrane and constructing a growth factor-sustained release system conforming to the tendon-healing cycle. The new materials were characterised, and the biological effects on tenocytes and fibroblasts were evaluated. The tendon injury model of New Zealand rabbits was constructed to observe the effects on tendon adhesion and healing.

**Results:** After freezing and vacuum drying, fresh amnions were found to effectively remove most of the cell components but retained the active components TGF- $\beta$ 1, bFGF, VEGF, and PDGF, as well as the fibrous reticular structure of the basement membrane. After coating with PCL nanofibres, a composite membrane mimicking the structure of the tendon sheath was constructed, thereby strengthening the tensile strength of the amnion. By up-regulating the phosphorylation of ERK1/2 and SMAD2/3, the adhesion and proliferation of tenocytes and fibroblasts were promoted, and collagen synthesis was enhanced. In the rabbit tendon repair model, the composite membrane effectively isolated the exogenous adhesion tissue and promoted endogenous tendon healing.

**Conclusion:** The composite membrane mimicking the structure of tendon sheath effectively isolated the exogenous adhesion tissue and achieved good tendon slip. By slowly releasing the growth factors TGF- $\beta$ 1, bFGF, VEGF and PDGF, the ERK1/2 and SMAD2/3 pathways were regulated. Consequently, endogenous tendon healing was promoted. This strategy can alternatively address the clinical problem of tendon adhesion.

**Keywords:** amniotic membrane, electrospinning, nanofibers, composite membrane, tendon adhesion

Correspondence: Dehu Tian  
Department of Hand Surgery, The Third Affiliated Hospital of Hebei Medical University, 139 Ziqiang Road, Shijiazhuang, Hebei 050017, People's Republic of China  
Tel +86-151-3056-6366  
Fax +86-311-8860-3818  
Email tiandehu\_1961@126.com

## Introduction

The formation of adhesion after tendon injury is a common clinical complication. Given the lack of effective adhesion prevention measures, treatment often falls into the vicious cycle of adhesion–release–adhesion, which seriously affects the

functional rehabilitation of patients.<sup>1</sup> In the United States, more than 320,000 cases of tendon injuries are caused by trauma and excessive exercise each year, resulting in billions of dollars in medical expenses. Moreover, 30–40% of patients have complications, such as limited joint activity due to tendon adhesion.<sup>2</sup> In this study, we focused on reducing the incidence of tendon adhesion and promoting the healing of the tendon.

Through an in-depth study of tendon structure and adhesion mechanism, researchers have explored various methods and materials for preventing tendon adhesion. The application of a physical barrier to block exogenous healing is currently the main method used in preventing tendon adhesion. Given the different physical and chemical properties of materials, their mechanisms of action and clinical effects vary.<sup>3,4</sup> The absorbable polymer compound polycaprolactone (PCL) has excellent biocompatibility, degradability and strong mechanical strength and is widely used in clinical practice.<sup>5,6</sup> However, the material is single and has no biological activity so it is not conducive to cell adhesion and proliferation. Thus, the material should be modified.<sup>7,8</sup>

Natural material amnion derived from living organisms has a semipermeable membrane and is rich in collagen, cytokines, enzymes and other active ingredients, allowing nutrient penetration. Moreover, its unique structure makes it an ideal biological material.<sup>9,10</sup> Clinical and basic research on amnion have been conducted for nearly 100 years. As early as 1913, Stem used amniotic membrane for repairing skin burns and ulcer wounds.<sup>11,12</sup> Advances and in-depth understanding of the biological characteristics of the amnion have been achieved recently. The human amniotic membrane has many cell growth factors, such as transforming growth factor (TGF- $\beta$ 1) and fibroblast growth factor (bFGF), vascular endothelial growth factor (VEGF) and platelet-derived growth factor (PDGF). These factors are important regulators for the repair of tendon injury and adhesion formation.<sup>13–16</sup> In clinical application, fresh amnion has safety hazards, cannot be preserved for a long time, lacks mechanical strength and dissolves very quickly, which causes slippage. To overcome these limitations of amniotic materials, researchers should introduce other materials or change the morphology of amnion should be changed to increase the convenience of application, improve the strength of the amnion, and moderate hydrophobicity for maximising the potential of amniotic materials.

With the development of nanotechnology, electrospinning technology is eliciting extensive attention. Nanomaterials prepared by electrospinning technology have a large specific surface area and high porosity and can construct a 3D network space structure similar to the natural extracellular matrix. It is one of the most influential technologies in the field of regenerative medicine in the 21st century.<sup>17,18</sup> In this study, fresh amnion was treated by freezing and vacuum drying. By utilising electrospinning technology, PCL nanofibres were coated onto the two surfaces of the freeze-dried amnion to form a multilayer composite membrane, and a growth factor-sustained release system was constructed to meet the tendon-healing cycle. This study aimed to optimise the amnion material and explain the mechanism of the interaction between tendon and amnion material.

## Materials and Methods

### Materials

#### Amniotic Membranes

This work followed the tenets of the Declaration of Helsinki involving human subjects and received approval from the Ethics Board of the Third Hospital of Hebei Medical University. Fresh amnion was provided by the Department of Obstetrics and Gynaecology, Third Hospital of Hebei Medical University. HBV, HCV, HIV, syphilis, and gonorrhoea were all negative in the maternal serological examination. The amnions were obtained after the consent form was signed by the pregnant woman and her family. Smooth and translucent amnions were obtained by passive separation between the amniotic membranes and chorionic membranes. The amnions were immersed in 50  $\mu$ g/mL penicillin and 50  $\mu$ g/mL streptomycin in a balanced salt solution for 20 min and placed in DMEM. Amnions were stored in a refrigerator at 4 °C and then set aside.

The fresh amnions were placed in the freeze dryer studio and frozen for 1–10 h at 0 °C–50 °C. The freezing chamber was opened to refrigerate until a cold trap temperature range of –10 °C to –56 °C. The vacuum pump was opened, and the water content ranged from 1% to 20%. Freeze-dried amnions were sterilised by cobalt 60 irradiation.

#### Electrospinning of Nanofibrous Membranes

Approximately 1 g of PCL (average Mn-80,000, Sigma-Aldrich) and 0.5 g of gelatine (Porcine skin, Vetec reagent grade, Type A) were dissolved in 10 mL of hexafluoroisopropanol (>98%, Shanghai Nortel Co., Ltd.) at room temperature and stirred by magnetic force. After

dissolving completely, the mixture was defoamed and stirred using a magnetic rod overnight. When the ambient temperature was 25 °C and humidity was 60%, the electrospinning device was connected. The electrospinning solution was placed into a 2 mL syringe with a needle diameter of 0.7 mm. The flow rate of the solution was adjusted to 1.0 mL/h, the voltage was set at 13 kV and the receiving distance was set at 15 cm. The PCL nanofibres were received on the two surfaces of freeze-dried amnions. The nanofibre membrane was dried overnight in a vacuum container for future use (Figure 1A).

## Characterization of the Electrospun Fibrous Membranes

The nanofibre membrane samples collected on aluminium foil were plated with gold for 90 s. The morphologies of the nanofibre membrane were observed by scanning electron microscopy (SEM) at an acceleration voltage of 10 kV. Image analysis software Image J was applied. The SEM images were analysed to calculate the diameter of 200 nanofibres.

The porosity of the nanofibre membrane was tested by ethanol permeation.<sup>19</sup> The nanofibre membrane was

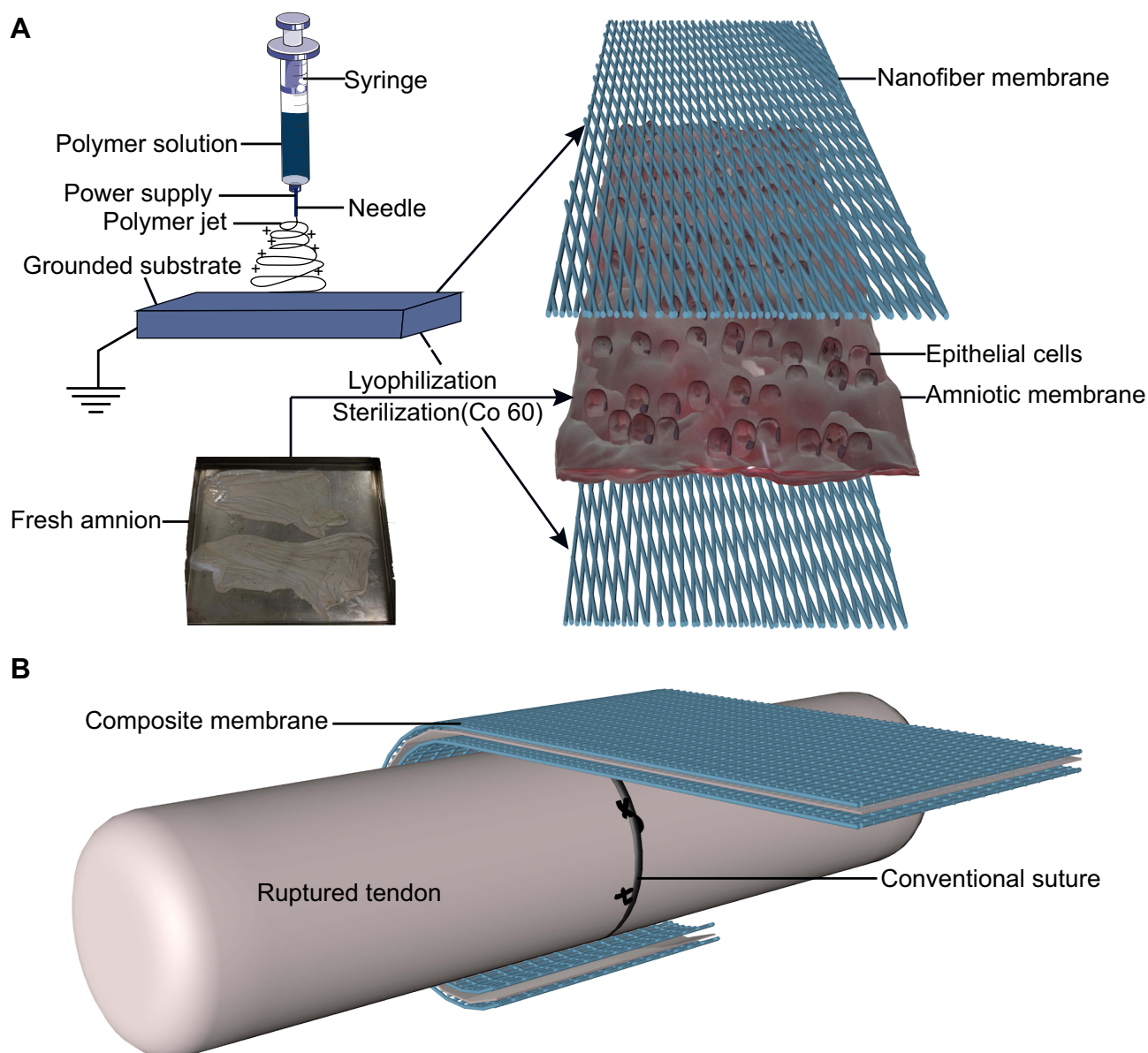


**Figure 1** (A) Polycaprolactone nanofibers prepared via electrospinning technology and fresh amnion after freeze-drying treatment constitute a multi-layer composite membrane. (B) Scheme of the nanofiber membrane wrapping ruptured tendon to prevent adhesion.

immersed in ethanol, and the volume of ethanol in the cylinder before and after the membrane was immersed was set to V1 and V2, respectively. After 15 min, the membrane was removed from ethanol, and the volume of the remaining ethanol was recorded as V3. The porosity of the test film was calculated according to the following equation:

$$\text{Porosity}(\%) = \left( \frac{V1 - V3}{V2 - V3} \right) \times 100\%$$

The water droplets were added dropwise on the surface of the sample for 10 s, and the hydrophilic angle of the freeze-dried amnion and nanofibre membranes was measured at 25 °C by using a hydrophilic angle metre and processed with DSA 1.8 software.

The stress-strain curve of the freeze-dried amnion and nanofibre membranes was measured. Five samples were obtained, and the size of the spline was 50.0 × 5.0 mm<sup>2</sup>. Both ends of the sample were placed on the two mechanical clamps of the mechanical measuring instrument (MTS-Exceed-Model E42, MTS Systems Corporation, USA). Exactly 3 mm of the sample was set aside as the test object. The tensile rate was 0.5 mm/s. The average value of the test results was obtained.

Freeze-dried amnions and nanofibre membranes were cut into 10 mm × 10 mm small pieces, immersed in saline for 15 min, fixed with 4% formaldehyde, embedded in paraffin for continuous sections (thickness of 5 microns), stained with HE and observed under light microscopy.

The surface microstructures of the freeze-dried amnions, polycaprolactone fibre membranes and nanofibre membranes were observed by SEM. The chemical composition and elemental distribution of the materials were analysed by X-ray energy dispersive spectrometry (EDAX, TEAM, USA). The energy spectrum test involved an acceleration voltage of 20 kV.

## In vitro Cell Experiment

### Isolation and Culture of Tenocytes and Fibroblasts

Male and female New Zealand white rabbits aged 6 months weighing 2.0–3.0 kg were provided by the Animal Laboratory Centre of the Third Hospital of Hebei Medical University. Under the ascending condition, sodium pentobarbital (30 mg/kg) was injected into the ear vein and fixed in the prone position, and the dorsal toe was incised. The flexor digitorum tendon and peritendinous tissue were harvested. The samples were washed three times with PBS containing double antibodies and placed in DMEM containing 0.1%

type II catabolic enzyme at 4 °C overnight. The specimens were cut into 1 mm<sup>3</sup> pieces by scissors and placed in DMEM containing 0.15% collagenase NB4. The mixture was shaken in a 37 °C isothermal shaker for 2 h. The residual tissue was filtered through a sterile filter and centrifuged at 200 g for 5 min, and the supernatant was discarded. The cell precipitate was suspended in DMEM containing 10% FBS and 1% birestance. Cell suspension was added to the culture dish. The culture dish was placed at 37 °C in 5% CO<sub>2</sub> and 95% air incubator. The liquid was changed 2–3 times a week in which half of the liquid was changed each time. The adherence, extension and cell growth were observed daily. When the cells proliferated and fused to 80%, they were subcultured in 1:2 bottles. The 3rd to 5th generations were used for experimental research.

### Evaluation of Cell Proliferation

The freeze-dried amnion and nanofibre membrane were placed in a 24-well plate, and another blank control group was used. Three groups were immersed in 75% alcohol for 1 h. The alcohol was aspirated and washed with PBS three times to remove residual alcohol. The tenocytes and fibroblasts were seeded on the material at a density of 5×10<sup>3</sup> cells/cm<sup>2</sup> and cultured in DMEM containing 10% FBS and 1% double antibody. Cells from different materials were digested with 0.25% trypsin on the 1st, 3rd, 5th, 7th, 10th and 15th days. Cell viability was detected by the cell counting kit-8 (CCK-8) method. The absorbance of each group was determined using an enzyme labelling instrument (measuring wavelength, 450 nm). The final absorbance value was obtained by subtracting the absorbance of the blank group. The growth curve was plotted with the number of culture days on the horizontal axis and the absorbance value on the vertical axis.

### Cell Fluorescence Staining and Adhesion Test

On the fifth day of cell culture, the cells were fixed with 4% paraformaldehyde solution for 10 min, washed twice with PBS and permeated with 200 pL of 0.1% Triton X-100 solution for 10 min. Triton X-100 solution was extracted, and 200 µL of phalloidin (20 µg/mL) was added to stain at room temperature for 30 min. Phalloidin was aspirated and washed twice with PBS, and the mixture was added with 200 µL of DAPI (1 µg/mL) for 5 min at room temperature in the dark. Confocal laser microscopy was used to observe cell adhesion, growth and cytoskeleton of different materials and obtain the images.



## Western Blot Analysis

Cell culture and grouping were conducted as previously described. Cells were collected on the 7th day after culture, and protein was extracted with cell lysate (20 mmol/L Hepes, pH 7.2, 1% Triton X-100, 10% triglyceride, 150 mmol/L NaCl, 1 mmol/L Na3OV4, 10 mg/L leupeptin and 1 mmol/L PMSF). The protein concentration of the cell was measured using the BCA protein assay kit (Beijing Solarbio Science & Technology Co., Ltd., China). The samples were electrophoresed through 8% SDS-PAGE gel and then transferred onto a PVDF membrane. After blocking with 5% non-fat milk, the membranes were incubated with antibodies against TGF- $\beta$ 1, bFGF, VEGF, PDGF, COL1, SMAD2/3, p-SMAD2/3, ERK1/2, P-ERK1/2 (Abcam, USA) and  $\beta$ -actin (Beijing Bioss Biotechnology Co., Ltd., China) overnight at 4 °C. After washing, the membranes were incubated with secondary antibodies (Abcam, USA) for 1 h. The membrane was washed with TBST buffer (50 mm Tris-HCl, 100 mm NaCl and 0.1% Tween 20, pH 7.4) three times and scanned with the Odyssey Fc System (LICOR, USA).

## Animal Experiment

All protocols of the animals were approved by the Ethics Board of the Third Hospital of Hebei Medical University, and the subject was conducted in accordance with the institutional guidelines for the care and treatment of animals.

A total of 81 adult New Zealand rabbits weighing 2.0–3.0 kg were randomly divided into the control, freeze-dried amnion and nanofibre membrane groups, with 27 rabbits in each group. Pentobarbital sodium (30 mg/kg) was injected into the ear vein and fixed in the prone position, and a 1.5 cm-long incision was made between the metatarsophalangeal joint of the third toe of the hind foot and proximal interphalangeal joint under sterile condition. The tendon sheath was excised, the flexor digitorum profundus tendon was transversely cut and the wound was sutured by the modified Kessler method. In the control group, the wound was sutured directly. In the two other groups, the freeze-dried amnion and nanofibre membrane were wrapped around the suture (Figure 1B). After the operation, the lower limbs were fixed, kept warm, moisture proofed and fed separately in a single cage to ensure adequate diet. Penicillin (400,000 U) was intramuscularly injected once a day for three consecutive days.

## Macroscopic and Microscopic Evaluation

Three weeks after the operation, nine animals in each group were killed by intravenous injection of excessive sodium

pentobarbital. The third toe was obtained to observe tendon healing and adhesion onto surrounding tissues. Tendon adhesion (macroscopic and microscopic) was evaluated on the basis of the criteria defined by Yang et al.<sup>20</sup>

Tendon adhesion was graded according to Yang's classification criteria as follows: grade 5, adherent tissues with an area of over 97.5% need sharp separation; grade 4, adherent tissues with an area of over 51–97.5% need sharp separation; grade 3, adherent tissues with an area of less than 50% need sharp separation; grade 2, adherent tissues can be bluntly separated; and grade 1, no adherent tissues. Histologic adhesions were classified as follows:<sup>21</sup> grade 4, severe (>66% of the tendon surface); grade 3, moderate (33–66% of the tendon surface); grade 2, mild (<33% of the tendon surface); and grade 1, no adhesions. Tendon healing was graded according to Tang's classification criteria as follows:<sup>22</sup> grade 4, poor (partial segregation of the tendon at suture site or proliferation of large amount of granulation tissue); grade 3, general (irregular collagen bundles in tendon, partially invaded by adhesion tissue); grade 2, good (collagen fibres in tendon showed good repair, but tendon sheath was invaded by adhesion tissue); and grade 1, excellent (continuous collagen fibres in tendon, smooth peritendon). The sections were observed blindly under light microscopy by two independent observers.

## Biomechanical Evaluation

The metacarpophalangeal joint was severed three weeks after the operation. The sliding distance, total flexion angle and maximum tensile strength of the tendon were measured using a biomechanical experimental machine. The proximal phalanges of toes were fixed on the experimental machine, and the retained flexor digitorum profundus tendon was tracted by 1 N force. The traction force was gradually increased to 10 N. The length of the tendon pulled away from the tendon sheath was marked and measured, and the total flexion angle (the sum of the flexion angles of proximal and distal interphalangeal joints) was measured and calculated using a goniometer. The tissue around the deep flexor tendon was removed, and the distal phalanx was preserved. The two ends of the deep flexor tendon were fixed on a biomechanical testing machine and moved at a speed of 20 mm/N until the tendon ruptured. The maximum tensile rupture strength of the tendon was simultaneously recorded.

## Statistical Analysis

The data were expressed as mean  $\pm$  standard deviation and analysed by one-way ANOVA with statistical software

SPSS 24.0 and Graphpad Prism 7. Statistical significance was considered at  $p < 0.05$ . Kruskal–Wallis test and post-hoc Bonferroni test were used to evaluate tendon adhesion. Bonferroni correction was used to reduce the chances of obtaining false-positive results because multiple pairwise tests were performed on a single set of data. To perform a Bonferroni correction, we divided the alpha ( $\alpha$ ) by the number of comparisons made. In our study, three groups and three pairwise comparisons were employed. Thus, we divided  $\alpha$  by 3. The statistical significance level for comparison was set at  $p < 0.016$ .

## Results

### Characterization of Electrospun Fibrous Membranes

SEM photographs showed that the freeze-dried amniotic epithelial cells were closely arranged with an intact structure, flat surface, slightly dry shrinkage and clear intercellular junction structure. The nanofibres were cylindrical, continuous, smooth and beadless, with an average diameter of  $475.4 \pm 147.5$  nm and porosity of  $77.0\% \pm 10.4\%$ . Under light microscopy, the freeze-dried amniotic epithelial cells were arranged tidily and tightly, with a thick and continuous basement membrane underneath. The amniotic membrane was coated with double-layer PCL nanofibres in the nanofibre membrane (Figure 2).

EDS analysis showed that the main components of lyophilised amniotic membrane were carbon (C), nitrogen (N), oxygen (O), sulphur (S), and phosphorus (P). Among them, N (15.52%) was the essential element of protein. PCL nanofibres were primarily composed of C and O. After composing the nanofibre composite membrane with lyophilised amnion, the elemental composition comprised N, P, S, chlorine (Cl) and a small amount of metal elements, which were primarily derived from the proteins in the inner amniotic membrane of the composite membrane. The uniform distribution of the elements in freeze-dried amnion indicated that the thickness of amnions was uniform, and the freeze-dried process did not cause amnion shrinkage. C and O in the PCL nanofibres were distributed along the circular distribution of porous fibres. This arrangement was beneficial to the nanofibre membrane, providing its porous structure and allowing the slow release of active proteins (Figure 3).

The hydrophilic angles of freeze-dried amnion and nanofibre membrane were  $51.18^\circ \pm 2.72^\circ$  and  $59.44^\circ \pm 4.15^\circ$ , respectively. Pressure–strain tests showed that the maximum

modulus of elasticity of the nanofibre membrane was higher than that of the freeze-dried amnion, and the tensile strength and toughness of the nanofibre membrane were higher than those of the freeze-dried amnion (Figure 4A).

### In vitro Cell Study

Tenocytes and fibroblasts were cultured for 1, 3, 5, 7, 10 and 15 days. The cells were counted by the CCK-8 method. The number of cells increased with time. No significant difference was observed in the activity of tenocytes among the three groups on the 1st and 3rd days. The cells in the freeze-dried amnion group and nanofibre membrane group grew rapidly, and their activities increased on the 5th, 7th, 10th and 15th days ( $p < 0.05$ ). The cell growth curve showed that the growth trend of cells in each group slowed down after seven days. In the first seven days, the growth trend of cells in the freeze-dried amnion group was high, and the growth trend of nanofibre membrane increased thereafter. Cell fluorescence staining showed that the number of cells in the freeze-dried amnion and nanofibre membrane groups was more than that in the control group at the same time point (Figure 4B and C).

The growth of tenocytes and fibroblasts on different materials was observed by confocal laser microscopy. The tenocytes and fibroblasts demonstrated good biocompatibility with freeze-dried amnion and nanofibre membrane. They were round or spindle shaped and evenly distributed on the surface of the material, exhibiting better growth activity than the control group (Figure 5).

### Western Blot

The expression levels of TGF- $\beta$ 1, bFGF, VEGF, PDGF, COL1, p-SMAD2/3 and P-ERK1/2 in the freeze-dried amnion group and nanofibre membrane group were higher than those in the control group. No significant difference was observed in the expression levels of SMAD2/3 and ERK1/2 (Figure 4D).

### Evaluation of Tendon Adhesion and Healing

Three weeks after the operation, the wounds healed well without infection or ulcer. Gross observation showed dense adhesions around the tendons in the control group, which required sharp separation. The amnion was difficult to recognise, and a small amount of fibrous tissue adhered between the tendons and surrounding tissues. Almost no adhesions were observed in the nanofibre membrane group (Figure 6).

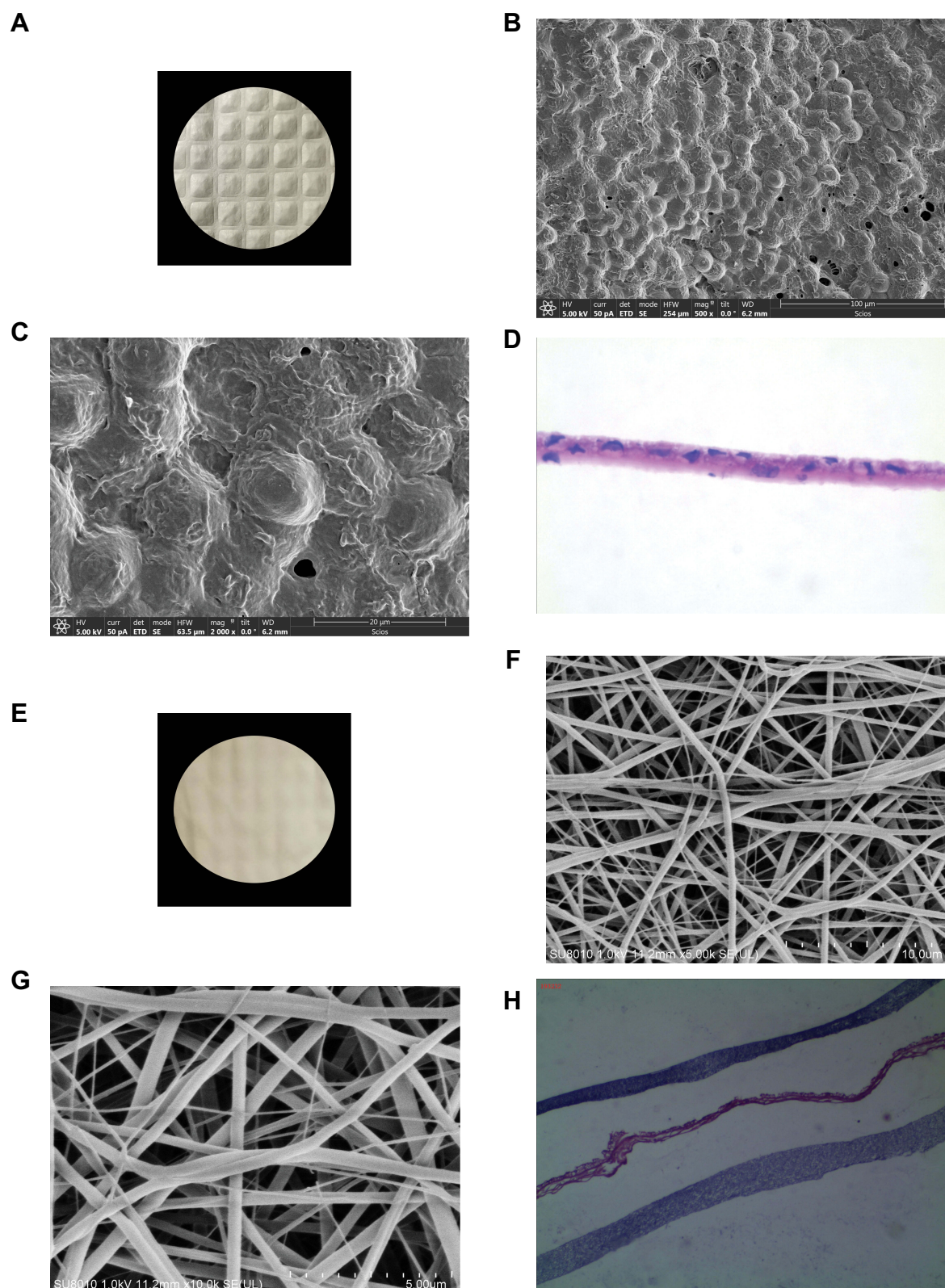


**Figure 2** General appearance of the freeze-dried amnion (A) and the nanofiber membrane (E). SEM images showing the surface morphology of the freeze-dried amnion and nanofiber membrane. Images of the freeze-dried amnion observed under SEM (B, C) and light microscopy (D); and images of the nanofiber membrane observed under SEM (F, G) and light microscopy (H).



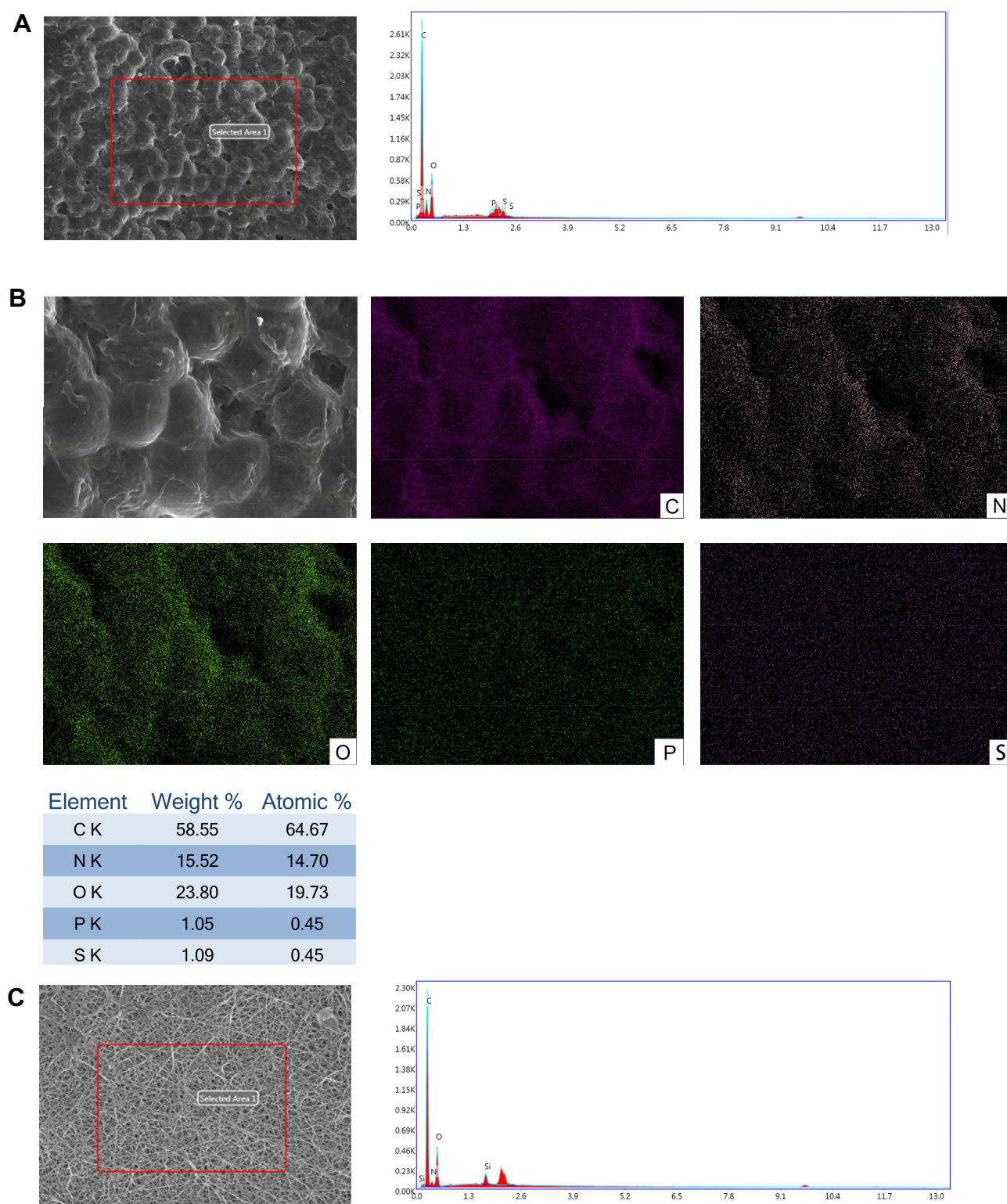


**Figure 3** X-ray energy spectrum analysis (EDS) of the freeze-dried amnion, PCL, and nanofiber membrane. The microstructure, EDS energy spectrum, and elemental composition of randomly selected regions of the freeze-dried amnion (**A**), PCL (**C**), and nanofiber membrane (**E**). Surface distribution of the main elements in the freeze-dried amnion (**B**), PCL (**D**), and nanofiber membrane (**F**).

In comparison with the histological sections of the repaired tendons in each group, serious adhesion was found between the tendons and surrounding tissues in

most of the samples of the control group. The broken ends of the tendons were separated, and many irregular collagen fibres were found. In the amnion group, the



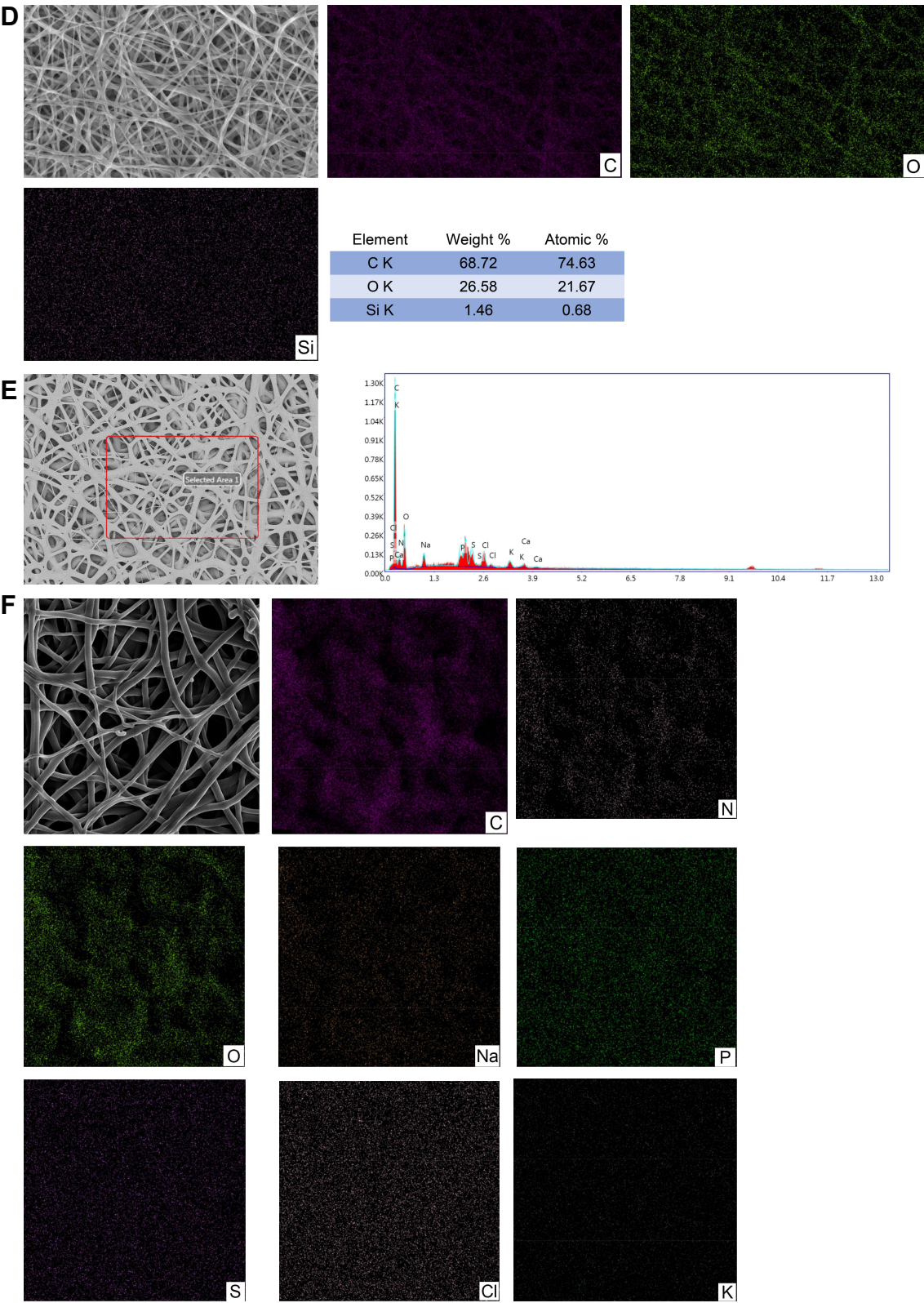


**Figure 3 (Continued).**

tendon healed well, but the tendon sheath was invaded by adhesion tissue, and loose fibrous tissue bundles were found with the surrounding tissue. In the nanofibre

membrane group, the peritendon was smooth, and almost no adhesion tissue was found. The histological parameters of tendon adhesion in the nanofibre membrane group were

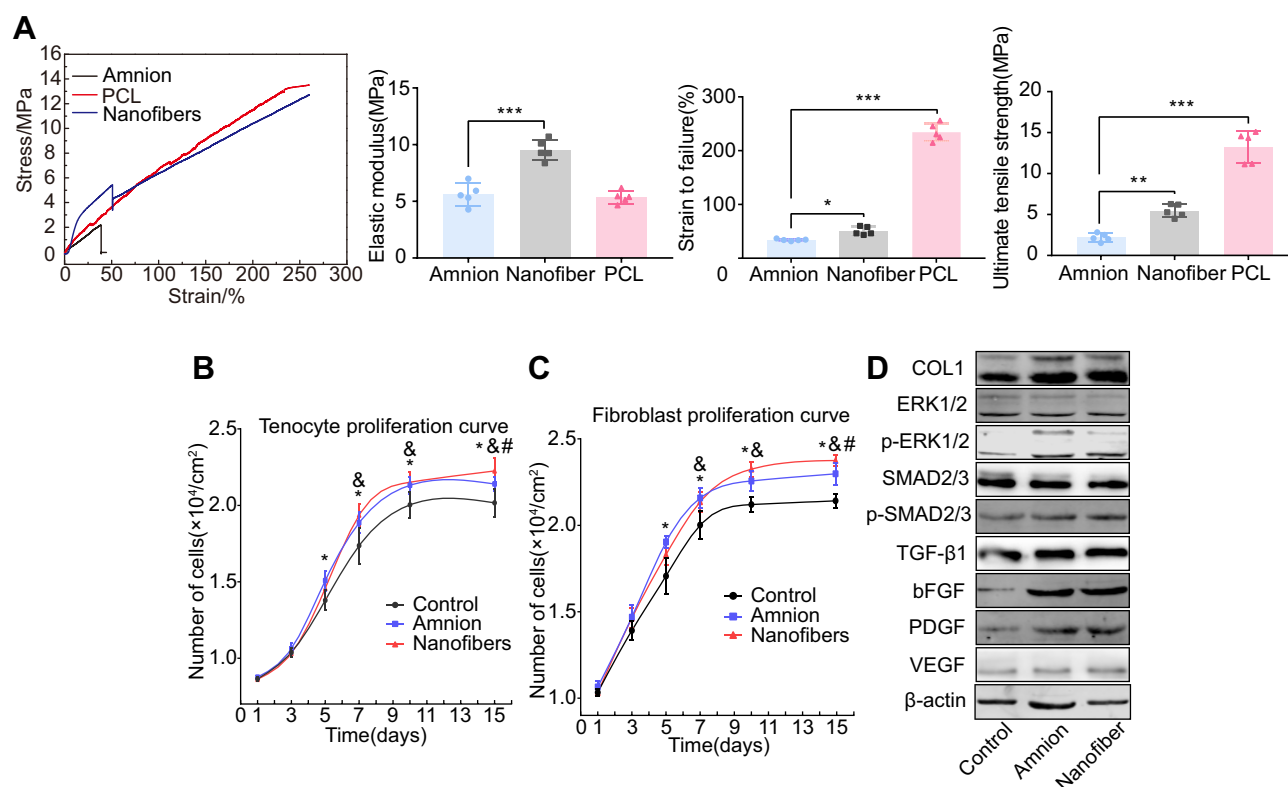


**Figure 4** (A) Mechanical properties of membranes. Stress-strain curves of the freeze-dried amnion and nanofibre membrane. Comparison of elastic modulus, strain to failure and ultimate tensile strength for the freeze-dried amnion and the nanofibre membrane. \* $p < 0.05$ ; \*\* $p < 0.01$ ; \*\*\* $p < 0.001$ . (B, C) Adhesion and proliferation of tenocytes and fibroblasts on the surface of the control group, freeze-dried amnion and nanofibre membrane were evaluated. \*The freeze-dried amnion group compared with the control group; #The nanofibre membrane group compared with the control group; #The nanofibre membrane group compared with the freeze-dried amnion group. Statistical difference was considered at  $p < 0.05$ . (D) On the 7th day of cell culture, the expression levels of TGF- $\beta$ 1, bFGF, VEGF, PDGF, COL1, SMAD2/3, p-SMAD2/3, ERK1/2 and P-ERK1/2 proteins in the control, freeze-dried amnion and nanofibre membrane groups were observed. The expression levels of TGF- $\beta$ 1, bFGF, VEGF, PDGF, COL1, p-SMAD2/3 and P-ERK1/2 in the freeze-dried amnion and nanofibre membrane groups were higher than those in the control group.

remarkably lower than those in the two other groups. The healing of the nanofibre membrane and amnion groups was significantly better than that of the control group ( $p < 0.016$ ; Figure 7A–C).

## Biomechanical Evaluation

At each time point after the operation, significant statistical differences were found in the tendon sliding distance and total flexion angle in the nanofibre membrane and amnion groups compared with those in the control group ( $p < 0.05$ ). The maximum tensile breaking strength of tendons in the nanofibre membrane group and amnion group was lower than that in the control group, but the difference was not significant (Figure 7D–F).

## Discussion

The amnion originates from the innermost layer of the placenta. The role of amnion in wound healing has been confirmed by many studies in the past 100 years, primarily through accelerating epithelialisation,<sup>23</sup> alleviating inflammation,<sup>24</sup>

inhibiting scar formation<sup>25</sup> and antimicrobial effects.<sup>26</sup> Although many studies have shown that the amnion has great potential in tissue repair, many shortcomings limit the maximisation of its potential in clinical applications. Fresh amnion cannot be preserved for a long time, which is inconvenient for clinical applications. It is very thin, has low mechanical strength and easy to tear; completely flat adhesion to the wound is difficult to ensure. Moreover, the therapeutic effect and mechanism of amnion in tendon repair have not been reported.

Most of the cell components in fresh amnion were effectively removed after freezing and vacuum drying, and the fibrous reticular structure of the basement membrane and dense layer was retained. After coating the PCL nanofibre onto the amniotic membrane, its strength increased. The 3D porous structure provided sufficient space for cell growth, which promoted the proliferation of tenocytes and fibroblasts, up-regulated the phosphorylation of ERK1/2 and SMAD2/3 and promoted the synthesis of type I collagen. The nanofibre composite membrane of



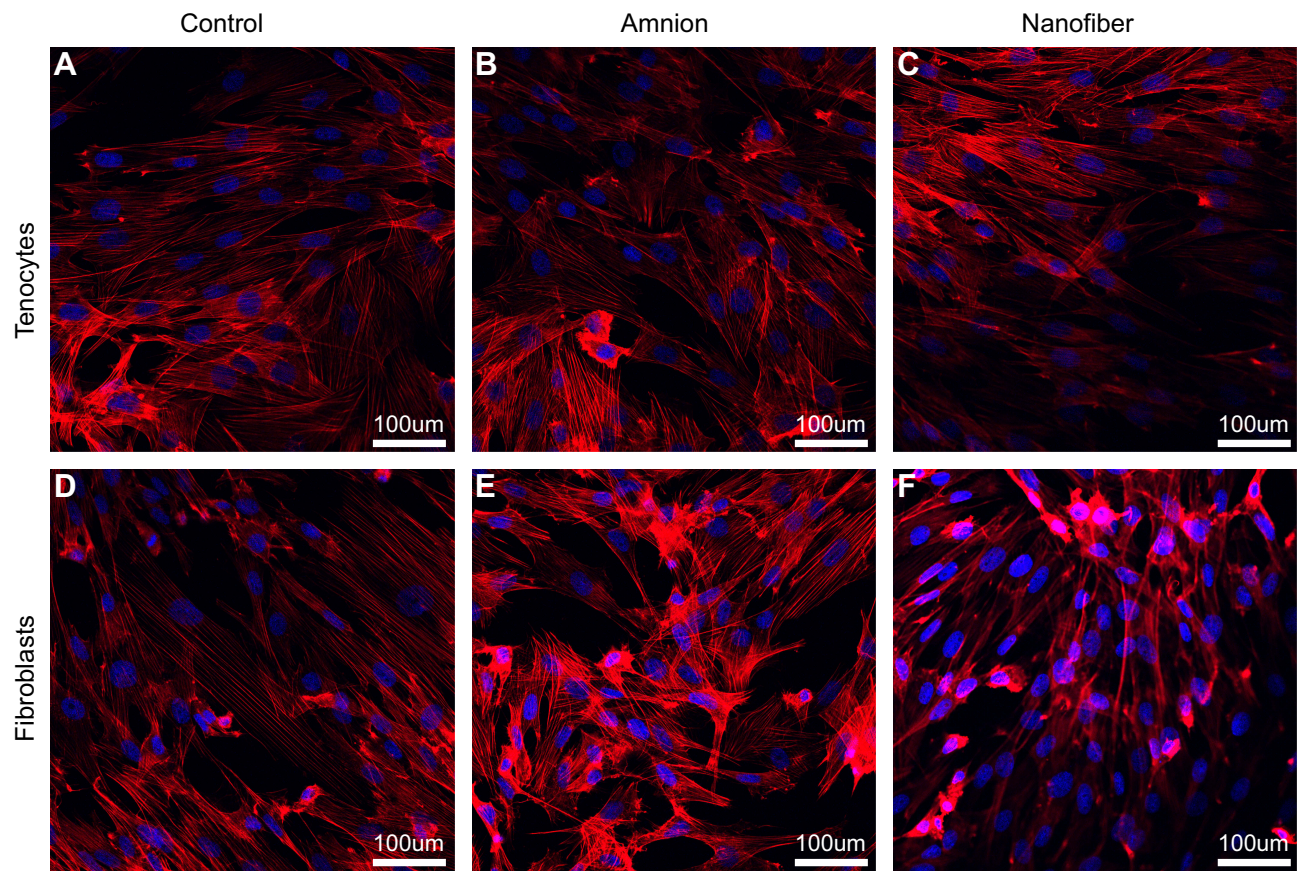


**Figure 5** Fluorescence images showing the cell morphology and the adhesion and proliferation of tenocytes (A–C) and fibroblasts (D–F) on the surface of the control group. The freeze-dried amnion and nanofiber membrane were observed after 5 days of culture. Tenocytes and fibroblasts presented a clear cytoskeleton, good biocompatibility with freeze-dried amnion and nanofiber membrane, and even distribution on the surface of the materials, showing better growth activity than the control group.

the porous structure slowly released bioactive components, such as TGF- $\beta$ 1 into the tendon repair area, which conformed to the tendon-healing repair cycle. In the rabbit model of tendon repair, compared with the control and amnion groups, the nanofibre membrane isolated the exogenous invasive tissue, promoted the endogenous healing of tendon and inhibited tendon adhesion.

The amnion is the abandoned placental tissue with a thickness of approximately 0.02–0.05 mm. It is the thickest basement membrane in the human body. It has a wide range of sources, low cost, low immunogenicity, no tumorigenicity and no ethical controversy, making it an ideal biological dressing. Clinical and basic research on the amnion has a long history. In 1913, Stem used amnion for skin burn and ulcer wound transplantation. Since then, the amnion has been widely used as dressing in ophthalmology, neurosurgery and gynaecology. The first problem encountered in the clinical application of amnion is its long-term preservation; hence, it should be used immediately. MiMedx Company obtained the commercial

amniotic membrane EpiFix by freezing and drying. Zelen found that EpiFix can substantially accelerate the healing rate of diabetic foot ulcers through randomised controlled clinical trials. Four weeks after the treatment, the wound healing rate of the EpiFix treatment group was 97.1%, which was higher than that of the standard treatment group (32%).<sup>27</sup> Freeze-dried amnion can preserve the structure of fresh amnion and is rich in various growth factors. Koob conducted ELISA that revealed that freeze-dried amnion expresses PDGF, TGF- $\beta$ 1, bFGF, EGF and GCSF, and these factors promote the proliferation and migration of fibroblasts.<sup>28</sup>

However, freeze-dried amnion is thin and has low mechanical strength. It is easily torn and difficult to spread completely to the wound during the operation. In this study, the mechanical strength of amnion was enhanced by the electrospinning of PCL. Considering the porous and large specific surface area and the various growth factors, collagen, laminin, fibronectin and proteoglycan in the amniotic matrix, nanofibres provide sufficient 3D space structure for cell growth and promote the



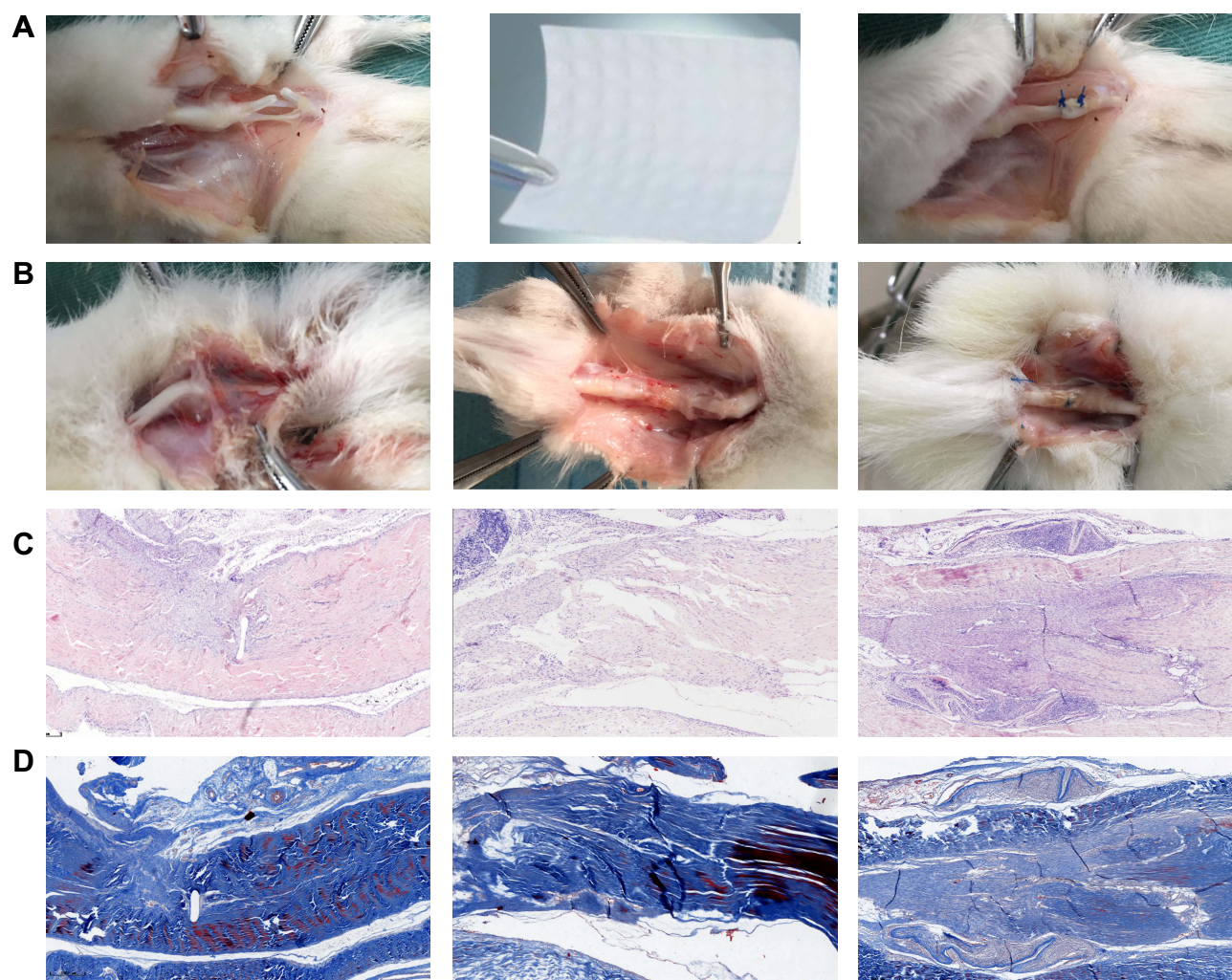


**Figure 6** (A) Photographs of the implantation site before and after wrapping with the nanofiber membrane. (B) Gross views of untreated tendons (control group), freeze-dried amnion, and nanofiber membrane with different levels of adhesion 3 weeks after operation. Histological analysis was performed to assess adhesion formation by using hematoxylin-eosin (C) and Masson's trichrome stains (D). Tendons are denoted by "T." The black triangle represents the adhesive tissue. The black arrow indicates the freeze-dried amnion and nanofiber membrane encapsulating the tendon repair area.

adhesion and proliferation of tenocytes and fibroblasts. The nanofibre membrane provides a suitable 3D space structure for cell growth. The amniotic matrix, similar to the human dermis, can be used as a natural carrier to provide an appropriate microenvironment to promote the adhesion, proliferation and differentiation of epidermal cells and fibroblasts. Choi used an amniotic matrix as scaffold to construct tissue-engineered skin, which survived well, and its structure was similar to that of normal skin.<sup>29</sup> Uberti found that the extract of amnion expresses PDGF, TGF- $\beta$ 1, bFGF, EGF and GCSF, which can promote the proliferation and migration of epidermal cells and fibroblasts, increase epithelialisation, accelerate dermal remodelling and enhance the healing of acute and chronic wounds.<sup>30</sup> These factors are important regulators of tendon repair and adhesion formation.

TGF- $\beta$ 1 promotes the synthesis of collagen in tendon cells and the expression of collagen I, fibronectin and  $\alpha$ -smooth muscle actin in tendon sheath fibroblasts. Fibroblasts, which are stimulated by TGF- $\beta$ 1, bFGF, PDGF and IGF, can proliferate and secrete collagen and produce a series of related inflammatory factors, such as tumour necrosis factor- $\alpha$ , interleukin-1 $\beta$ , interleukin-6 and prostaglandin, which further aggravate inflammation and cause tissue adhesion.<sup>31</sup> The key physiological processes, such as proliferation, migration and differentiation, are regulated by intracellular signal transduction, and the activation of ERK1/2 and SMAD2/3 is crucial. Heldin found that TGF- $\beta$ 1 and TGF- $\beta$  type II receptors bind to form a complex that promotes the phosphorylation of SMAD2/3 and enhances the transcription of target genes, such as collagen.<sup>32,33</sup> Zhao found that amnion contains several



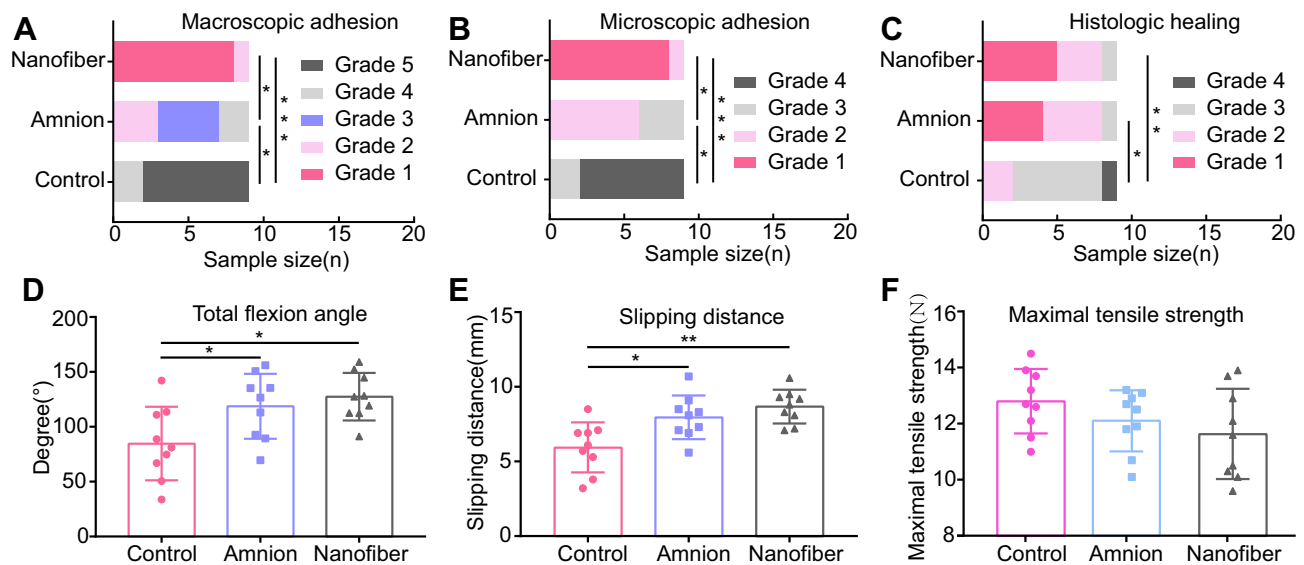


**Figure 7** At 3 weeks after operation, the adhesion and healing quality were evaluated based on gross observation (A), histological analysis (B, C), flexion angle of interphalangeal joint (D), tendon sliding distance (E), and maximum tensile fracture strength (F). \* $p < 0.016$ ; \*\* $p < 0.005$ ; \*\*\* $p < 0.001$ .

growth factors, namely, bFGF and PDGF, which promote keratinocyte proliferation by activating the MEK/ERK and PI3K/Akt signal transduction pathways.<sup>34,35</sup>

The amnion and nanofibre composite membrane promoted the expression of growth factors, such as TGF- $\beta$ 1, bFGF, PDGF and VEGF and up-regulated the phosphorylation of ERK1/2 and SMAD2/3 but did not affect the expression of ERK1/2 and SMAD2/3. Therefore, bFGF, PDGF and VEGF stimulated the proliferation of tenocytes and fibroblasts through the RAS-MEK-ERK pathway, whereas TGF- $\beta$ 1 stimulated the secretion of collagen and other products by tenocytes and fibroblasts through the SMAD pathway.

Tendon healing is closely related to tendon adhesion. Adhesion primarily occurs because fibroblasts grow from the surrounding tissue to the broken end of the tendon during exogenous healing and form adhesion between the tendon and surrounding tissue. Endogenous healing is mediated by tenocytes, which primarily promote the healing of broken tendon ends. Therefore, understanding how to control exogenous healing and promote endogenous healing can address the problem of tendon adhesion and improve the quality of tendon healing.<sup>36</sup>

Blocking exogenous healing by a physical barrier primarily prevents tendon adhesion. Non-degradable materials, such as polyethylene, can prevent adhesion in the initial stage, but the foreign body reaction caused by nonabsorption and subsequent adhesion persists.<sup>37</sup> PCL nanofibres

have attracted increasing attention because of their excellent mechanical properties and structure similar to the extracellular matrix. Feng prepared PCL fibrous membranes through electrospinning technology to prevent cardiac surgery adhesion in rabbit models. Results showed that the membranes can inhibit fibroblast infiltration, possess sufficient mechanical strength, have good biocompatibility and effectively resist sternal and epicardial adhesion.<sup>7</sup> However, most of the current antiadhesion membranes have no biological activity, and they can only isolate the invasion of adhesion tissue but fail to simultaneously promote tendon self-healing. Thus, their effect is limited.

The tendon sheath wrapped around the tendon is an important structure for maintaining tendon slip and nutrition. It consists of the outer fibrous sheath, inner synovial sheath and synovial fluid (mainly hyaluronic acid) between the two layers.<sup>38</sup> Tendon sheath is not only a good biological barrier to prevent the invasion of surrounding tissues, but it also provides nutrition and promotes tendon healing.<sup>39,40</sup> In this study, PCL nanofibres, as the outer layer, functioned as a natural tendon sheath to prevent fibroblasts and other tissues from invading. The amniotic membrane, as the intermediate layer, can promote tendon endogenous healing by releasing bioactive substances, such as TGF- $\beta$ 1, bFGF, PDGF and VEGF, which can diffuse into the repair site through the pore of the nanofibrous membrane and enhance the proliferation of tenocytes and collagen synthesis. PCL nanofibres acted

as the inner layer to maintain tendon slip through their proper hydrophilicity and smoothness (Figure 8). The experimental results of the rabbit tendon injury model showed that the nanofibre composite membrane, which imitated the structure of natural tendon sheath, effectively isolated the exogenous adhesion tissue and achieved good tendon sliding.<sup>41,42</sup>

PCL nanofibres completely enveloped the AM through physical action without extrusion or crosslinking and retained the biological activity of the proteins to the greatest extent. Zhou et al constructed a composite membrane containing a single layer of PCL and AM.<sup>43,44</sup> The

physical extrusion and the acrylic acid that led to the binding of activated carboxy and AM may reduce the protein activity.<sup>45</sup> Moreover, the edge of the AM reinforced by monolayer PCL was easy to rise. Leppänen wrapped the repaired flexor tendon with commercial lyophilised AM.<sup>46</sup> Compared with the control group, no significant functional improvement was achieved. The main reason was that the AM material directly enveloped the tendon that not only promoted the accelerated healing of the tendon but also aggravated the adhesion between the AM and the peritendinous tissue. Therefore, the PCL between AM and repaired tissue is very important.

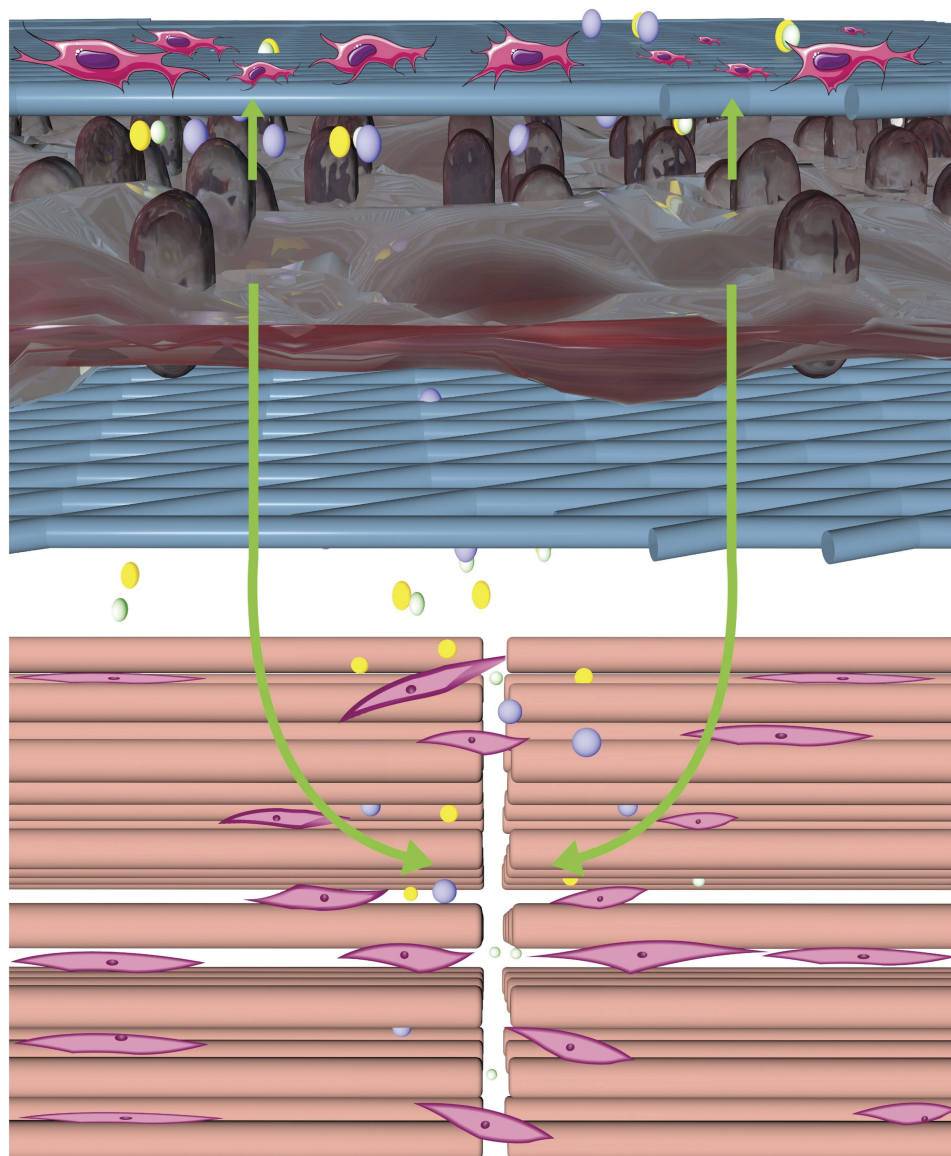


**Figure 8** Mechanism of nanofiber composite membrane that promotes endogenous healing of tendon and prevents exogenous adhesion. The inner layer of freeze-dried amnion contains several active factors, such as TGF- $\beta$ 1, bFGF, VEGF, and PDGF. These factors are slowly released to the tendon repair area through the porous network structure of PCL nanofibers, which promotes the proliferation of tenocytes and the synthesis of collagen. The outer layer of PCL nanofibers functions as a barrier to fibroblasts and other exogenous tissue invasion.

This study showed that the prepared nanofibre composite membrane efficiently prevented tendon adhesion, but some improvements are necessary. The PCL/GT electrospun fibre membranes with a ratio of 2:1 were prepared in this study, which showed good effects in preventing tendon adhesion. Considering that the ratio of PCL/GT may lead to different mechanical properties, degradation and biocompatibility, we will study the various PCL/GT ratios in the future. The nanofibre composite membrane avoided the shortcomings of using an amniotic membrane or PCL nanofibre membrane alone. The long-term tendon healing and antiadhesion effects after complete degradation need to be confirmed by further experiments. We observed that the amniotic membrane increased the phosphorylation of ERK1/2 and SMAD2/3 through various active factors, thereby promoting the proliferation of tenocytes, fibroblasts and collagen synthesis. The ERK and SMAD signal pathways are primarily involved in the pathological process of tendon healing and adhesion formation, but the specific mechanism of how the two pathways interact with each other remains unclear. Only Western blot analysis was performed without other means of verification: this limitation is exactly what this study needs to improve. Therefore, these problems require follow-up research.

## Conclusion

In this experiment, fresh amniotic membranes were treated by freezing and vacuum drying, which effectively removed most of the cell components but retained the active components, such as TGF- $\beta$ 1, bFGF, VEGF, PDGF and the basement membrane layer of the fibrous reticular structure. After coating with PCL nanofibres, a composite membrane mimicking the structure of tendon sheath was constructed that strengthened the tensile strength of the amniotic membrane, increased the phosphorylation of ERK1/2 and SMAD2/3, promoted the proliferation of tenocytes and enhanced collagen synthesis. In the rabbit model experiment, the nanofibre composite membrane effectively isolated exogenous adhesion tissue and promoted the endogenous healing of tendons. This study provides a new treatment strategy to address the clinical problem of tendon adhesion and has broad application prospects.

## Acknowledgments

This work was supported by a grant (H2019206388) from the Hebei Province National Science Foundation.

## Disclosure

The authors report no conflicts of interest in this work.

## References

- Jiang S, Zhao X, Chen S, et al. Down-regulating ERK1/2 and SMAD2/3 phosphorylation by physical barrier of celecoxib-loaded electrospun fibrous membranes prevents tendon adhesions. *Biomaterials*. 2014;35(37):9920–9929. doi:10.1016/j.biomaterials.2014.08.028
- Butler DL, Juncosa-Melvin N, Boivin GP, et al. Functional tissue engineering for tendon repair: a multidisciplinary strategy using mesenchymal stem cells, bioscaffolds, and mechanical stimulation. *J Orthop Res*. 2008;26(1):1–9. doi:10.1002/(ISSN)1554-527X
- Chen SH, Chou PY, Chen ZY, Lin FH. Electrospun water-borne polyurethane nanofibrous membrane as a barrier for preventing post-operative peritendinous adhesion. *Int J Mol Sci*. 2019;20:7.
- Li L, Zheng X, Fan D, et al. Release of celecoxib from a bi-layer biomimetic tendon sheath to prevent tissue adhesion. *Mater Sci Eng C Mater Biol Appl*. 2016;61:220–226. doi:10.1016/j.msec.2015.12.028
- Goh BT, Teh LY, Tan DB, Zhang Z, Teoh SH. Novel 3D polycaprolactone scaffold for ridge preservation—a pilot randomised controlled clinical trial. *Clin Oral Implants Res*. 2015;26(3):271–277. doi:10.1111/clr.12486
- Unagolla JM, Jayasuriya AC. Enhanced cell functions on graphene oxide incorporated 3D printed polycaprolactone scaffolds. *Mater Sci Eng C Mater Biol Appl*. 2019;102:1–11. doi:10.1016/j.msec.2019.04.026
- Feng B, Wang S, Hu D, et al. Bioresorbable electrospun gelatin/polycaprolactone nanofibrous membrane as a barrier to prevent cardiac postoperative adhesion. *Acta Biomater*. 2019;83:211–220. doi:10.1016/j.actbio.2018.10.022
- Gupta D, Venugopal J, Prabhakaran MP, et al. Aligned and random nanofibrous substrate for the in vitro culture of Schwann cells for neural tissue engineering. *Acta Biomater*. 2009;5(7):2560–2569. doi:10.1016/j.actbio.2009.01.039
- Cunningham BW, Seiber B, Riggleman JR, Van Horn MR, Bhat A. An investigational study of a dual-layer, chorion-free amnion patch as a protective barrier following lumbar laminectomy in a sheep model. *J Tissue Eng Regen Med*. 2019;13:1664–1671.
- Kim JT, Kim KW, Mun SK, Chun YS, Kim JC. Transplantation of autologous perichondrium with amniotic membrane for progressive scleral necrosis. *Ocul Surf*. 2019. doi:10.1016/j.jtos.2019.05.004
- Amer MI, Abd-El-Maeoud KH, Abdelfatah I, Salama FA, Abdallah AS. Human amnion as a temporary biologic barrier after hysteroscopic lysis of severe intrauterine adhesions: pilot study. *J Minim Invasive Gynecol*. 2010;17(5):605–611. doi:10.1016/j.jmig.2010.03.019
- Hassan M, Prakasam S, Bain C, Ghoneima A, Liu SS. A randomized split-mouth clinical trial on effectiveness of amnion-chorion membranes in alveolar ridge preservation: a clinical, radiologic, and morphometric study. *Int J Oral Maxillofac Implants*. 2017;32(6):1389–1398. doi:10.11607/jomi.5875
- Kim SW, Zhang HZ, Kim CE, Kim JM, Kim MH. Amniotic mesenchymal stem cells with robust chemotactic properties are effective in the treatment of a myocardial infarction model. *Int J Cardiol*. 2013;168(2):1062–1069. doi:10.1016/j.ijcard.2012.11.003
- Vosdoganes P, Wallace EM, Chan ST, Acharya R, Moss TJ, Lim R. Human amnion epithelial cells repair established lung injury. *Cell Transplant*. 2013;22(8):1337–1349. doi:10.3727/096368912X657657
- Han VK, Bassett N, Walton J, Challis JR. The expression of insulin-like growth factor (IGF) and IGF-binding protein (IGFBP) genes in the human placenta and membranes: evidence for IGF-IGFBP interactions at the feto-maternal interface. *J Clin Endocrinol Metab*. 1996;81(7):2680–2693. doi:10.1210/jcem.81.7.8675597
- Fu Q, Ohnishi S, Sakamoto N. Conditioned medium from human amnion-derived mesenchymal stem cells regulates activation of primary hepatic stellate cells. *Stem Cells Int*. 2018;2018:4898152. doi:10.1155/2018/4898152



17. Feng Y, Wang Q, He M, et al. Antibiofouling zwitterionic gradational membranes with moisture retention capability and sustained antimicrobial property for chronic wound infection and skin regeneration. *Biomacromolecules*. 2019;20(8):3057–3069. doi:10.1021/acs.biomac.9b00629
18. Lv C, Chen S, Xie Y, et al. Positively-charged polyethersulfone nanofibrous membranes for bacteria and anionic dyes removal. *J Colloid Interface Sci*. 2019;15(556):492–502. doi:10.1016/j.jcis.2019.08.062
19. Yin H, Wang J, Gu Z, et al. Evaluation of the potential of kartogenin encapsulated poly(L-lactic acid-co-caprolactone)/collagen nanofibers for tracheal cartilage regeneration. *J Biomater Appl*. 2017;32(3):331–341. doi:10.1177/0885328217717077
20. Yang DJ, Chen F, Xiong ZC, Xiong CD, Wang YZ. Tissue anti-adhesion potential of biodegradable PELA electrospun membranes. *Acta Biomater*. 2009;5(7):2467–2474. doi:10.1016/j.actbio.2009.03.034
21. Güzdemir E, Ekşioğlu F, Korkusuz P, Aşan E, Gürsel İ, Hacırcı V. Chondroitin sulfate-coated polyhydroxyethyl methacrylate membrane prevents adhesion in full-thickness tendon tears of rabbits. *J Hand Surg Am*. 2002;27(2):293–306. doi:10.1053/j.hsu.2002.31161
22. Tang JB, Shi D, Zhang QG. Biomechanical and histologic evaluation of tendon sheath management. *J Hand Surg Am*. 1996;21(5):900–908. doi:10.1016/S0363-5023(96)80212-7
23. Niknejad H, Peirovi H, Jorjani M, Ahmadiani A, Ghanavi J, Seifalian AM. Properties of the amniotic membrane for potential use in tissue engineering. *Eur Cells Mater*. 2008;7:88–99. doi:10.22203/eCM
24. Thiex NW, Chames MC, Loch-Carus RK. Tissue-specific cytokine release from human extra-placental membranes stimulated by lipopolysaccharide in a two-compartment tissue culture system. *Reprod Biol Endocrinol*. 2009;7:117. doi:10.1186/1477-7827-7-117
25. Solomon A, Wajngarten M, Alviano F, et al. Suppression of inflammatory and fibrotic responses in allergic inflammation by the amniotic membrane stromal matrix. *Clin Exp Allergy*. 2005;35(7):941–948. doi:10.1111/cea.2005.35.issue-7
26. Kjaergaard N, Hein M, Hyttel L, et al. Antibacterial properties of human amnion and chorion in vitro. *Eur J Obstet Gynecol Reprod Biol*. 2001;94(2):224–229. doi:10.1016/S0301-2115(00)00345-6
27. Zelen CM, Serena TE, Snyder RJ. A prospective, randomised comparative study of weekly versus biweekly application of dehydrated human amnion/chorion membrane allograft in the management of diabetic foot ulcers. *Int Wound J*. 2014;11(2):122–128. doi:10.1111/iwj.2014.11.issue-2
28. Koob TJ, Rennert R, Zabek N, et al. Biological properties of dehydrated human amnion/chorion composite graft: implications for chronic wound healing. *Int Wound J*. 2013;10(5):493–500. doi:10.1111/iwj.2013.10.issue-5
29. Choi JS, Kim JD, Yoon HS, Cho YW. Full-thickness skin wound healing using human placenta-derived extracellular matrix containing bioactive molecules. *Tissue Eng Part A*. 2013;19(3–4):329–339. doi:10.1089/ten.TEA.2011.0738
30. Uberti MG, Pierpont YN, Ko F, et al. Amnion-derived cellular cytokine solution (ACCS) promotes migration of keratinocytes and fibroblasts. *Ann Plast Surg*. 2010;64(5):632–635. doi:10.1097/SAP.0b013e3181c39351
31. Vermeulen S, Vasilevich A, Tsiapalis D, et al. Identification of topographical architectures supporting the phenotype of rat tenocytes. *Acta Biomater*. 2019;83:277–290. doi:10.1016/j.actbio.2018.10.041
32. Moustakas A, Souchelnytskyi S, Heldin CH. Smad regulation in TGF- $\beta$  signal transduction. *J Cell Sci*. 2001;114(Pt 24):4359–4369.
33. Heldin CH, Miyazono K, Ten Dijke P. TGF-beta signalling from cell membrane to nucleus through SMAD proteins. *Nature*. 1997;390(6659):465–471. doi:10.1038/37284
34. Zhao B, Liu JQ, Zheng Z, et al. Human amniotic epithelial stem cells promote wound healing by facilitating migration and proliferation of keratinocytes via ERK, JNK and AKT signaling pathways. *Cell Tissue Res*. 2016;365(1):85–99. doi:10.1007/s00441-016-2366-1
35. Katz M, Amit I, Yarden Y. Regulation of MAPKs by growth factors and receptor tyrosine kinases. *Biochim Biophys Acta*. 2007;1773(8):1161–1176. doi:10.1016/j.bbamcr.2007.01.002
36. Snedeker JG, Follen J. Tendon injury and repair - A perspective on the basic mechanisms of tendon disease and future clinical therapy. *Acta Biomater*. 2017;63:18–36. doi:10.1016/j.actbio.2017.08.032
37. Hsu SH, Dai LG, Hung YM, Dai NT. Evaluation and characterization of waterborne biodegradable polyurethane films for the prevention of tendon postoperative adhesion. *Int J Nanomedicine*. 2018;13:5485–5497. doi:10.2147/IJN.S169825
38. Yagi M, Sato N, Mitsui Y, Gotoh M, Hamada T, Nagata K. Hyaluronan modulates proliferation and migration of rabbit fibroblasts derived from flexor tendon epitenon and endotenon. *J Hand Surg Am*. 2010;35(5):791–796. doi:10.1016/j.jhsa.2010.02.010
39. Harrison RK, Mudera V, Grobbelaar AO, Jones ME, McGrouther DA. Synovial sheath cell migratory response to flexor tendon injury: an experimental study in rats. *J Hand Surg Am*. 2003;28(6):987–993. doi:10.1016/S0363-5023(03)00380-0
40. Xu L, Cao D, Liu W, Zhou G, Zhang WJ, Cao Y. In vivo engineering of a functional tendon sheath in a hen model. *Biomaterials*. 2010;31(14):3894–3902. doi:10.1016/j.biomaterials.2010.01.106
41. Liu S, Wu F, Gu S, et al. Gene silencing via PDA/ERK2-siRNA-mediated electrospun fibers for peritendinous antiadhesion. *Adv Sci*. 2018;6(2):1801217. doi:10.1002/adv.201801217
42. Zhang W, Li X, Comes Franchini M, et al. Controlled release of curcumin from curcumin-loaded nanomicelles to prevent peritendinous adhesion during Achilles tendon healing in rats. *Int J Nanomedicine*. 2016;22(11):2873–2881.
43. Zhou Z, Long D, Hsu CC, et al. Nanofiber-reinforced decellularized amniotic membrane improves limbal stem cell transplantation in a rabbit model of corneal epithelial defect. *Acta Biomater*. 2019;1(97):310–320. doi:10.1016/j.actbio.2019.08.027
44. Liu H, Zhou Z, Lin H, et al. Synthetic nanofiber-reinforced amniotic membrane via interfacial bonding. *ACS Appl Mater Interfaces*. 2018;10(17):14559–14569. doi:10.1021/acsami.8b03087
45. Greim H, Ahlers J, Bias R, et al. Assessment of structurally related chemicals: toxicity and ecotoxicity of acrylic acid and acrylic acid alkyl esters (acrylates), methacrylic acid and methacrylic acid alkyl esters (methacrylates). *Chemosphere*. 1995;31(2):2637–2659. doi:10.1016/0045-6535(95)00136-V
46. Leppänen OV, Karjalainen T, Göransson H, et al. Outcomes after flexor tendon repair combined with the application of human amniotic membrane allograft. *J Hand Surg Am*. 2017;42(6):474.e1–474.e8. doi:10.1016/j.jhsa.2017.03.006

## International Journal of Nanomedicine

### Publish your work in this journal

The International Journal of Nanomedicine is an international, peer-reviewed journal focusing on the application of nanotechnology in diagnostics, therapeutics, and drug delivery systems throughout the biomedical field. This journal is indexed on PubMed Central, MedLine, CAS, SciSearch®, Current Contents®/Clinical Medicine,

Journal Citation Reports/Science Edition, EMBASE, Scopus and the Elsevier Bibliographic databases. The manuscript management system is completely online and includes a very quick and fair peer-review system, which is all easy to use. Visit <http://www.dovepress.com/testimonials.php> to read real quotes from published authors.

Submit your manuscript here: <https://www.dovepress.com/international-journal-of-nanomedicine-journal>